Electrical charging of aerosol nanoparticles and some practical applications(·)

M. Alonso*, A. Hernández-Sierra* and F.J. Alguacil*

Abstract

This review article summarizes the main results of recent fundamental research on the electrical charging of nanometer-sized aerosol particles (particle diameter below 10 nm, Knudsen number above about 15, kinetic regime). It covers topics of great relevance to aerosol processing and measurement, such as the effect of the presence of a number of ions on the surface of a nanoparticle on its electrical mobility; the experimental measurement of charging probability / efficiency for particle diameter below 10 nm, both for diffusion and corona discharge type chargers; the effect of particle growth by Brownian coagulation on the charging process; and the examination of after-charging effects downstream of an aerosol neutralizer. The last part of this article discusses two practical applications of nanoaerosol charging, namely, the particle size measurement by electrical methods, and some electrostatic effects on the removal of nanoparticles from gas streams.

Keywords

Aerosol nanoparticles. Electrical charging. Kinetic regime. Differential mobility analyzer. Nanoparticle removal.

Cargado eléctrico de partículas de aerosol en régimen cinético y algunas aplicaciones prácticas

Resumen

El presente artículo es una revisión bibliográfica sobre el cargado eléctrico de aerosoles de nanopartículas (diámetro de partícula inferior a 10 nm, número de Knudsen mayor de 15, régimen cinético). El artículo abarca algunos tópicos de gran interés para el procesado y la medición de aerosoles, tales como el efecto de la presencia de iones en la superficie de la nanopartícula en su movilidad eléctrica; la medición experimental de probabilidad / eficacia de cargado para partículas de diámetro inferior a 10 nm, tanto para cargadores de tipo difusivo como para los de descarga de corona; el efecto del crecimiento de partícula por coagulación browniana en el proceso de cargado; y los efectos de post-cargado corriente abajo del neutralizador. En la parte final del artículo, se analizan someramente dos aplicaciones prácticas del cargado eléctrico de nanoaerosoles, a saber, la medición del tamaño de partícula por métodos eléctricos, y algunos efectos electrostáticos en el proceso de eliminación de partículas en efluentes gaseosos.

Palabras clave

Aerosol de nanopartículas. Cargado eléctrico. Régimen cinético. Analizador diferencial de movilidad. Eliminación de nanopartículas.

1. INTRODUCTION

The study of nanometer aerosols has already become a central activity in a variety of scientific and technological fields[1]. For instance, the gas-to-particle conversion process[2 and 3] is currently an efficient method to produce controlled-size nanoparticles used in the preparation of high-purity functional materials with special mechanical, optical, electric or magnetic properties. Another field where nanoparticles suspended in a gas medium is of particular importance is Environmental Engineering: nanoparticles practically pass uncaptured through most of the conventional particle collection equipments presently available, and this creates severe problems[4], because of several reasons: nanoparticles can remain in suspension in the atmosphere for longer periods of time and be transported to longer distances far away from the emission point; condensation of toxic gaseous species takes place preferentially onto the surface of

nanoparticles because these have a comparatively very large specific surface area[5-11]; and nanometer-sized particles are precisely those which, due to their high diffusivity, penetrate and deposit most easily into our lungs[12-14]. Therefore, alternative equipments must be designed and developed to ensure proper removal of the smallest particles present in gas exhausts. In particular, it should be of great interest to devise high-efficiency electric chargers for nanoparticles so that they can be subsequently collected by electrostatic precipitation.

In whatever case, knowledge of the particle size distribution of nanoaerosols constitutes an unavoidable requirement. In the particle size range of a few nanometers, the most accurate sizing technique to date is the electrostatic classification[15]. In this method, the aerosol particles must be previously charged, usually in a radioactive ionizer or in a corona discharge type charger, though an alternative method employing X-rays is being currently studied[16]. To avoid particle detection problems, it is desirable to have a concentration of charged particles as high as possible at the outlet of the charging chamber. This goal becomes harder to achieve for smaller particles, because of their higher wall deposition rate and lower charging probability. Normally, the process of charging and diffusion to the walls are accompanied by Brownian coagulation, whereby a further loss of small particles occurs. Moreover, the processes of diffusion to the walls and Brownian coagulation result in a modification of the original aerosol particle size distribution. Therefore, the charging process, which might seem of secondary importance at first glance, is actually a crucial step in the size measurement of aerosols by electrical techniques.

The present review is basically devoted to the examination of the most recent experimental results and theoretical developments in the field of nanoaerosol charging. The presence of electrical charges on the particles also affects other processes, favorably in some instances (e.g., filtration), not so favorably in others (e.g., measurement errors in particle sizing instrumentation). Some considerations concerning the mechanism of particle charging will be discussed first. Next, the charging probability / efficiency of nanoaerosols in unipolar and bipolar chargers will be examined, with and without simultaneous particle size growth by coagulation. The last two sections of this review will deal with particle size measurement in electrical mobility analyzers, and with the electrostatic enhancement of aerosol filters.

2. MECHANISM OF PARTICLE CHARGING

In the conventional charging process, a population of neutral aerosol particles is made to flow through a cloud of unipolar or bipolar ions. Ions diffuse toward the particles and collide with them. Upon collision, there are in principle two possible ways by which the particle can acquire a charge: (a) either ions physically attach to the surface of the particle, or (b) there is an exchange of electrons between the particle and the impinging ion. For the specific case of charging of an aerosol particle P by a positive ion I^+, one can represent schematically the two different mechanisms as:

$$P + I^+ \rightarrow (PI^+) \qquad \text{(ion attachment)} \qquad (1),$$

$$P + I^+ \rightarrow P^+ + I \qquad \text{(electron transfer)} \qquad (2),$$

where (PI^+) indicates the particle having the (whole) ion adsorbed onto its surface, P^+ represents an aerosol particle which has lost one electron, and I denotes a neutralized ion.

To decide which of the two mechanisms, if any, is correct, the following argument is proposed. If the particle P is very small, having a dimension of the same order of magnitude as that of the ions, the ion-attachment mechanism should modify the (electrical mobility equivalent) size of the particle. This size change should be detectable after several ions have attached to the aerosol particle. Indeed, if mechanism (1) is correct, the neutralization of charged aerosol particles should follow the following scheme:

$$(PI^+) + I^- \rightarrow (PI^+I^-) \qquad \text{(ion attachment)}, \qquad (3)$$
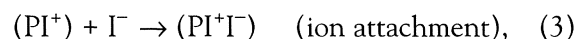
where the right-hand side denotes a particle with two attached ions of different polarity, giving a globally neutral particle. Further charging and neutralization would finally result in a particle having a certain number of positive and negative ions attached to its surface, which could be represented as $[P(I^+)_m(I^-)_n]$. Now, if the original mobility of P is very close to that of the ions, the difference in mobilities between P and $[P(I^+)_m(I^-)_n]$ should be detectable.

On the contrary, according to the model (2), the aerosol neutralization mechanism would be:

$$P^+ + I^- \rightarrow P + I \quad \text{(electron transfer)}, \qquad (4)$$

so that after consecutive charging and discharging steps, the final charged particle would simply be P^+ or P^- and there would be no mobility shift in this case.

The expected mobility shift (if the ion attachment mechanism is the correct one) is admittedly very small and, in fact, it should be too small to be measurable in the case of particles larger than about 4 or 5 nm – the mobility equivalent diameter of air ions is in the range 1-1.5 nm. Even for smaller aerosol particles, one would need a highly sensitive experimental set-up to detect these minute variations. Two differential mobility analyzers connected in series can serve this purpose if proper operating conditions are chosen and if a sensitive and reliable particle detecting and counting system is used.

A few years ago, we developed such an experimental system and improved its sensitivity to examine the occurrence or absence of a mobility shift as a consequence of consecutive charging-neutralization stages. The details of the experimental system and the experimentation method can be found in the original publication[17]. Careful experiments of successive charging and neutralization were carried out for aerosol particles of mobility equivalent diameter around 3 nm. The results of the exhaustive experimentation showed that particle mobility did not suffer any modification at all after several stages of charging and neutralization. This result favors the electron transfer as the mechanism of charging and neutralization of aerosol particles by ions, and it is also very important in other respect: it demonstrates the absence of any effect of the ion size on the particle-size distribution measured by a differential mobility analyzer even in the extreme case in which ions and particles have dimensions of the same order of magnitude.

3. CHARGING EFFICIENCY IN A BIPOLAR ION ENVIRONMENT

As already stated, the most reliable method presently available of nanoaerosol particle size measurement is the electrical mobility analysis. This technique requires previous charging of the particles and precise knowledge of the resulting charge distribution. The latter is needed to transform the experimentally measured electrical mobility distribution into the desired particle size distribution.

3.1. The charging equations in the absence of diffusion losses and coagulation

The system to be considered consists of an aerosol stream flowing through a container in which monovalent bipolar air ions are continuously generated, by radiation alpha or beta emitted by a radioactive source, at a rate g (number of ion pairs per unit time and unit volume). Denoting by $f_m^j(t)$, the fraction of particles that, at time t, have acquired m net charges of polarity j, the particle number conservation equation is simply:

$$f_0 + \sum_{m=1}^{\infty} \left(f_m^+ + f_m^- \right) = 1 \qquad (5),$$

where f_0 stands for the fraction of neutral particles.

The number concentration n^j of singly-charged ions of polarity j evolves with time according to the expression (see, for instance, references[18] and [19] among many others):

$$\frac{dn^j}{dt} = g - \alpha n^j n^k -$$

$$- Nn^j \left[\eta_0^{j0} f_0 + \sum_{m=1}^{\infty} \left(\eta_m^{jj} f_m^j + \eta_m^{jk} f_m^k \right) \right], \quad j, k = +,- \qquad (6)$$

where α is the ion recombination rate constant, and η_m^{jk} is the attachment rate coefficient of an ion of polarity j with a particle carrying m net charges of polarity k ($k = 0$ for neutral particles). Similarly, the temporal variation of the particle charge distribution is given by:

$$\frac{df_m^j}{dt} = n^j \left(\eta_{m-1}^{jj} f_{m-1}^j - \eta_m^{jj} f_m^j \right) + n^k \left(\eta_{m+1}^{kj} f_{m+1}^j - \eta_m^{kj} f_m^j \right),$$

$$j, k = +,-; \ m \geq 0 \qquad (7)$$

Equations (5)-(7) are supplemented with the charge conservation equation,

$$n^+ - n^- + N \sum_{m=1}^{\infty} m \left(f_m^+ - f_m^- \right) = \frac{\rho}{e}, \qquad (8),$$

where ρ is the initial space charge (i.e., before aerosol particles are let into the chamber), and e is the elementary charge.

The general system of balance equations (5-8) has no analytical solution. The steady state

solution can be found by assuming a fixed ion ratio, and by application of the principle of detailed balancing. According to this principle[20 and 21], the steady state rate at which particles of charge m capture positive ions is equal to the rate at which particles of charge $m + 1$ capture negative ions, that is,

$$\eta_m^{jk} n^j f_m^{*k} = \eta_{m+1}^{kj} n^k f_{m+1}^{*j} \qquad (9)$$

(The asterisc indicates steady state condition.) From (5) and (9), one finds the steady-state fraction of particles carrying m net charges of polarity j :

$$f_m^{*j} = \frac{\left(\dfrac{n^j}{n^k}\right)^m \prod_{p=1}^{m} \dfrac{\eta_{p-1}^{jj}}{\eta_p^{kj}}}{1 + \sum_{q=1}^{\infty}\left[\left(\dfrac{n^j}{n^k}\right)^q \prod_{p=1}^{q} \dfrac{\eta_{p-1}^{jj}}{\eta_p^{kj}} + \left(\dfrac{n^k}{n^j}\right)^q \prod_{p=1}^{q} \dfrac{\eta_{p-1}^{kk}}{\eta_p^{jk}}\right]} \qquad (10)$$

For relatively large particles (continuum regime) there exist analytical expressions for the ion attachment rate coefficients η_m^{jk} as a function of particle size[21 and 22] and, therefore, (10) gives the analytical expression for the steady-state distribution of charges on the aerosol particles as a function of the ionic ratio n^+ / n^- and the particle size. This theoretical charge distribution is commonly used in differential mobility analysis to infer the original particle size distribution from the measured mobility distribution. In practical aerosol particle size measurements one employs a sufficiently large charging chamber (and / or sufficiently low aerosol flow rate) so that the required steady-state time is amply exceeded. However, this practice may lead to erroneous results because, due to particle size distribution modification in the charger by diffusion losses and coagulation (the rates of which depend on particle size), the inferred particle size distribution may differ substantially from that of the original aerosol entering the charger.

In the special case of nanometer-sized aerosol particles, an analytical solution of the transient charging equations is possible, because some simplifying approximations are permissible. In the first place, the attachment rate coefficient between an ion of either polarity and a singly charged particle of the same polarity is practically zero for particle diameters below about 20 nm[18].

Therefore, for this range of particle size, the number concentration of particles with two or more net charges is negligible or even zero. Furthermore, the ion attachment rate coefficient between an ion and a neutral particle (charging coefficient) is extremely small, much smaller (between one and two orders of magnitude, depending on particle size) than the corresponding attachment rate coefficient between a charged particle and an ion of opposite polarity (discharging or neutralization coefficient). As a consequence, the number concentration of singly charged particles at the steady-state is but a very small fraction of the total aerosol number concentration, and this implies, first, that the fraction of ions spent in charging is negligible in comparison with ion losses by recombination and, second, that the equilibrium ion concentration existing in the charger before the aerosol is let in remains practically constant during the charging process. In this manner, the aerosol charging equations (7) decouple from the ion equations (6), and an analytical solution to the transient charging process is then possible.

For bipolar diffusion charging of nanoparticles, only four attachment rate coefficients are needed, η^{+0} and η^{-0} for charging of neutral particles and η^{+-} and η^{-+} for neutralization of singly charged particles. (The subscripts denoting the number of charges in the particle will be omitted, since a particle can acquire at most one net charge.) The ion-pair equilibrium number concentration in the charging chamber at time $t = 0$, just at the time when the aerosol stream is let in, is given by the steady-state solution of (6) without the charging-discharging terms:

$$n_{eq}^+ = n_{eq}^- = \sqrt{g / \alpha} = n \qquad (11)$$

Due to the different mobilities of positive and negative air ions, the attachment rate coefficients depend on the ion polarity and, as a consequence, for any time $t > 0$, the concentrations of positive and negative ions differ from each other. However, as explained above, the fraction of the equilibrium ion-pair concentration which is spent in charging or neutralization is so small that one can safely assume a constant ion-pair concentration throughout the process. In a sense, it is not that equation (7) decouples from (6), but simply that the latter is not needed to be considered at all to find the transient solution of the aerosol charging equations.

Under these special, but physically sound and of practical importance, circumstances, the aerosol charging equations become:

$$\frac{df^j}{dt} = n\eta^{j0} f^0 - n\eta^{kj} f^j, \quad j,k = +,-\quad (12)$$

The particle number conservation equation is simply

$$1 = f^0 + f^+ + f^-\quad (13)$$

The system of the two coupled equations (12) can be decoupled by transforming them into second order differential equations. The final solution is (see the original publication[23] for details):

$$f^j = f^{*j} + \frac{(n\eta^{j0} + m_1 f^{*j})\exp(m_2 t) - (n\eta^{j0} + m_2 f^{*j})\exp(m_1 t)}{m_2 - m_1}\quad (14),$$
$$j, k = +,-$$

where m_1 and m_2 are the roots of the equation $m^2 + Am + B = 0$:

$$m_1 = -\frac{1}{2}A\left(1 + \sqrt{1 - 4B/A^2}\right),$$
$$(15)$$
$$m_2 = -\frac{1}{2}A\left(1 - \sqrt{1 - 4B/A^2}\right)$$

and:

$$A = n (\eta^{+0} + \eta^{-0} + \eta^{+-} + \eta^{-+}),\quad (16)$$

$$B = n^2 (\eta^{+0}\eta^{+-} + \eta^{-0}\eta^{-+} + \eta^{+-}\eta^{-+})\quad (17)$$

(To avoid confusion, the superscripts of the attachment rate coefficients have been written down explicitly in the last two equations.)

In equation (14),

$$f^{*j} = \frac{n^2}{B}\eta^{j0}\eta^{jk}, \quad j, k = +,-\quad (18)$$

is the stationary charge distribution which, using (17), can also be written as:

$$f^{*j} = \frac{R^j}{1 + R^j + R^k}, \quad j, k = +,-\quad (19)$$

where,

$$R^j = \frac{\eta^{j0}}{\eta^{kj}}, \quad j, k = +,-\quad (20)$$

is the particle charging-to-discharging rate ratio. The same result (19) can be directly obtained by setting $df^j / dt = 0$ in (12).

Equation (14) gives the transient particle charge distribution and, as such, can be used in differential mobility analysis to transform the measured mobility distribution into the corresponding particle size distribution upon knowledge of the mean aerosol residence time in the charger. If wished, it can also be used to determine the time required to achieve the stationary distribution – strictly speaking, the stationary distribution is attained at $t \rightarrow \infty$, but an estimation, useful for practical purposes, can be done as follows.

The time-scale to reach the steady state can be found directly from the transient solution (14). Since there appear two exponential terms in this equation, actually there are two possible values (quite close to each other) for the time-scale τ, namely, $-1/m_1$ and $-1/m_2$. However, in the particle size range of interest (2-20 nm), $|m_1| > |m_2|$, so that it is the root m_2 the one that controls the approach to the stationary state. Therefore, the time-scale to attain the steady-state can be estimated by the expression:

$$\tau = -1/m_2\quad (21)$$

Obviously, this time-scale must be considered valid only within the particle size range where the solution (14) is valid, i.e., for particles below about 20 nm. For larger particles one can use the formulation of Mayya and Sapra[24], which is claimed to be valid for the entire particle size range (free-molecular, transition and continuum regimes).

3.2. Determination of the ion attachment rate coefficients

In the continuum regime (aerosol particles much larger than the ionic mean free path), the theory of the diffusion of ions to particles is based on the solution of the diffusion equation for ions in the electric field of a charge particle[20, 25 and 26], and analytical expressions for the attachment rate coefficients η^{jk} can be obtained. However, as we

have seen, the solution of the transient charging equations must be found by numerical methods.

In contrast, for nanometer-sized aerosol particles (kinetic or free molecular regime) we have been able to obtain an analytical solution of the transient charging equations, but analytical expressions for the ion attachment rate coefficients are not available. The calculation of the attachment rate coefficients is based on Fuchs theory[27], two recent good reviews of which can be found in references[18] and [28]. According to this theory, the space surrounding a particle is divided into two regions by a limitting sphere, concentric with the particle and having a radius in the order of one ionic mean free path larger than the particle radius. In the region outside the limitting sphere, ions move according to the continuum diffusion equation, whereas in the inner region they move as in a vacuum, without colliding with air molecules and following free-molecular transport trajectories. By matching the kinetic and continuum ion fluxes at the limitting sphere, the following equation is finally obtained:

$$\eta = \frac{\pi\delta^2\bar{c}\beta \exp[-\phi(\delta)/kT]}{1+\exp[-\phi(\delta)/kT][\delta^2\bar{c}\beta/4D]\int\limits_0^1 \exp[\phi(D_p/2x)/kT]dx} \quad (22)$$

In this equation, δ is the radius of the limitting sphere, which depends on the particle size and on the ionic mean free path. $\bar{c} = \sqrt{8kT/\pi m}$ and $D = kTZ/e$ are, respectively, the mean thermal velocity and diffusion coefficient of an ion with mass m and electric mobility Z. β is the collision probability, which depends on the electrostatic potential energy, ϕ, of an ion in the field of the particle:

$$\phi(r) = \frac{e^2}{4\pi\varepsilon_0}\left[\frac{p}{r} - \frac{\varepsilon-1}{\varepsilon+2}\frac{D_p^3}{16r^2(r^2-D_p^2/4)}\right] \quad (23),$$

where r is the distance measured from the centre of the particle of diameter D_p and dielectric constant ε, and ε_0 is the dielectric constant of a vacuum. In the above equation, $p = 0$ for a neutral particle, $p = 1$ if the ion and the singly charged particle have the same polarity and $p = -1$ if the charges on the ion and the particle are of opposite signs.

Upon knowledge of the ions properties (mass, mobility) one can determine numerically with equation (22) the values of the four different attachment coefficients as a function of particle

diameter. For practical purposes, regression analysis can then be carried out to obtain fitted $\eta(D_p)$ functions.

Actually, in the absence of any reliable relationship between ion mass and mobility, it has been a common practice among aerosol researchers to leave these two ionic properties as a sort of fitting parameters whose values can, to a certain extent, be freely chosen so as to match the predictions of Fuchs' theory with the experimental results. In past experimental works on particle charging[18, 29-36], ions were in all cases generated from the ionization of air molecules by alpha or beta radiation. The composition of the ions, and hence their physical properties, mainly depends on their age and on the nature of the trace compounds present in the air[28] and, hence, it is possible that the "air ions" differed from work to work. However, it seems unlikely that ion masses and mobilities could be so different from each other in these works (see references [28] and [36] for the whole collection of m and Z values assumed by a number of authors).

Using typical ionic masses of $m^+ = 150$ and $m^- = 80$ amu, and typical electrical mobilities of $Z^+ = 1.15$ and $Z^- = 1.65$ cm^{2}V^{-1}s^{-1}, we have calculated the ion attachment rate coefficients with equation (22) for the particle diameter range between 2 and 20 nm. The numerically calculated attachment rate coefficients are well reproduced by the following expressions:

$$\eta^{+0} = 2.19\times10^{-9}\,D_p^{1.51} \quad (24)$$

$$\eta^{-0} = 3.02\times10^{-9}\,D_p^{1.51} \quad (25)$$

$$\eta^{+-} = (5.68+3.38D_p-0.522D_p^2+0.042D_p^3-$$
$$-0.0017D_p^4+0.000027D_p^5)\times10^{-7} \quad (26)$$

$$\eta^{-+} = (2.15+4.20D_p-0.526D_p^2+0.038D_p^3-$$
$$-0.0014D_p^4+0.000020D_p^5)\times10^{-7} \quad (27),$$

where η is expressed in cm^{3}s^{-1} and D_p in nm.

Alternative theories to calculate the ion attachment coefficients have been proposed, all of them based on the concept of limitting sphere, but removing some of the simplifications assumed by Fuchs. Thus, Marlow and Brock[19] took into account the Maxwellian velocity distribution of approaching ions far from the particle; Hoppel and

Frick[18] included three-body trapping as a further mechanism of ion capture; and, more recently, Filippov[37] considered collisions between ions and neutral molecules inside the limitting sphere. These alternative charging theories give practically the same predictions as those of Fuchs', in spite that the latter is much more simple, in the particle diameter range above about 2 nm. Large discrepancies between Fuchs' theory and those of Marlow-Brock and Filippov appear for particle diameters below 2 nm but, unfortunately, in this extremely small particle size range there are no experimental data available which permit us deciding which of the proposed theories is correct.

3.3. Simultaneous charging and Brownian coagulation

The theoretical development summarized in the preceeding section is valid for sufficiently diluted aerosols and a sufficiently short residence time of the particles in the charging chamber. Under these special conditions, particle losses and particle size distribution modification due to diffusional deposition and Brownian coagulation may be neglected. On the contrary, the larger the residence time and/or the aerosol concentration, the larger the extent of dissapearance of the smaller particles.

Therefore, in the general case, i.e. in the presence of coagulation and diffusion to the walls, the particle size distribution changes with time and the analytical solution of the charging equations is no longer possible. If one only considers charging and diffusion losses, it is clear that there must exist an optimum residence time at which the concentration of charged particles is a maximum, and beyond which the population of charged particles decreases because the process of diffusion losses to the wall is steadily occurring from the beginning. When coagulation enters into play, the process is considerably more complex, because now particles of a given size are being lost by diffusion and by coagulation, but they are also being generated by coagulation of smaller particles. In this case too there must exist an optimum residence time for each particle size at which concentration is a maximum.

Charging experiments with highly concentrated nanoaerosols were performed by the aerosol research group of Osaka, where one of the authors spent a few years[38]. Since the original particle number concentration was quite high,

coagulation effects were much larger than diffusional losses, so that the latter could be neglected. Under these circumstances, the charging equations become:

$$\frac{dN_j^+}{dt} = \eta_j^{+0} n N_j^0 - \eta_j^{-+} n N_j^+ +$$

$$+ \Delta ln D_p \sum_{i=1}^{j-1} K_{i,j-i} N_i^0 N_{j-i}^+ - \sum_{i=1}^{\infty} N_j^+ (K_{i,j} N_i^0 + K_{i,j}' N_i^-) \quad (28),$$

$$\frac{dN_j^-}{dt} = \eta_j^{-0} n N_j^0 - \eta_j^{+-} n N_j^- + \quad (29),$$

$$+ \Delta ln D_p \left[\sum_{i=1}^{j-1} K_{i,j-i} N_i^0 N_{j-i}^- - \sum_{i=1}^{\infty} N_j^- (K_{i,j} N_i^0 + K_{i,j}' N_i^+) \right]$$

$$\frac{dN_j^0}{dt} = \eta_j^{+-} n N_j^- + \eta_j^{-+} n N_j^+ - \eta_j^{-0} n N_j^0 - \eta_j^{+0} n N_j^0 +$$

$$+ \Delta ln D_p \left[\sum_{i=1}^{j-1} 1/2 \ K_{i,j-i} N_i^0 N_{j-i}^0 + \sum_{i=1}^{j-1} K_{i,j-i}' N_i^+ N_{j-i}^- - \right.$$

$$\left. - \sum_{i=1}^{\infty} K_{i,j} N_j^0 (N_i^0 + N_i^- + N_i^+) \right] \quad (30)$$

where $N_j^0 \Delta ln D_p$, $N_j^+ \Delta ln D_p$ and $N_j^- \Delta ln D_p$ are, respectively, the number concentration of uncharged, positive and negative particles with diameter in the range between D_{pj} and $D_{pj} + \Delta ln D_p$; $K_{i,j}$ is the coagulation rate constant between particles of diameters D_{pi} and D_{pj} in the case that at most one of the colliding particles is charged. $K_{i,j}'$ is the rate constant for the coagulation of two charged particles of opposite polarity. The coagulation between charged particles of equal polarity is neglected because the corresponding rate constant is extremely low. In the above equations, the size index $j-i$ denotes particles with diameter $D_{pj-i} = (D_{pj}^3 - D_{pi}^3)^{1/3}$. The terms involving the coagulation of charged particles of opposite polarity, $K_{i,j}' N_i^+ N_j^-$, in equations (28)-(30) are comparatively much smaller than those involving collisions between uncharged particles, and between charged and uncharged particles, because the concentration of charged particles at any instant is at most 5 % of the concentration of uncharged particles. In the above equations, only the singly-charged particles need to be considered because, as already mentioned before, nanoparticles with two or more net charges of a given polarity are practically (or even totally) absent.

The experiments were carried out with radioactive tubular chargers of different volumes in order to examine the effect of residence time on the charging of a polydisperse population of aerosol nanoparticles. Typical results are shown in figure 1. The mismatch between theory and experiment at large residence time may be a consequence of having neglected diffusion losses: since the smaller particles are lost by diffusion to the charger walls more rapidly than the larger ones, their depletion rate is actually larger than indicated by the calculations. In any case, it is important to note that for each particle size there exists an optimum residence time in the charger, i.e. a time at which the output concentration of charged particles is a maximum. Clearly, one must design the charger and/or select the operating conditions very carefully in order to maximize the production of charged particles of a desired size. For instance, a large output concentration of very small particles requires a quite short residence time, much shorter than that required to attain the steady-state (equilibrium) charging condition[38].
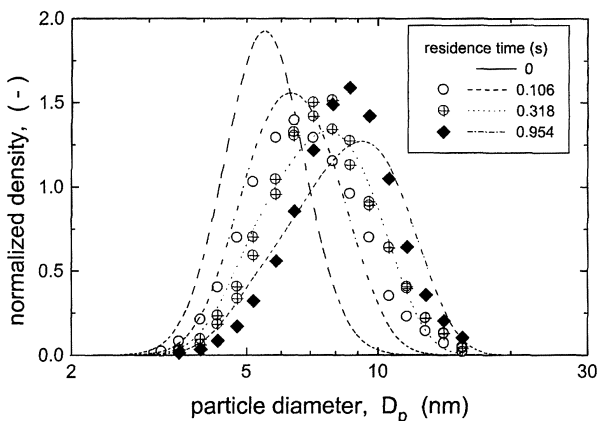
Figure 1. Typical time evolution of the particle size distribution in a diffusion-type charger. The line without symbol is the experimentally measured size distribution of uncharged particles at the charger inlet (zero residence time). The data points are experimental values of normalized density of negatively charged particles at different mean aerosol residence times in the charger. The discontinuous curves are distributions of negative particles obtained from numerical integration of equations (28)-(30).

Figura 1. Ejemplo típico de la evolución de la distribución de tamaño de partícula en un cargador de tipo difusivo. La curva sin símbolos corresponde a la distribución de partículas neutras medida experimentalmente a la entrada del cargador (tiempo de residencia cero). Los símbolos representan datos experimentales de densidad normalizada de partículas cargadas negativamente a diferentes valores del tiempo medio de residencia en el cargador. Las otras tres curvas han sido obtenidas por integración numérica de las ecuaciones (28)-(30).
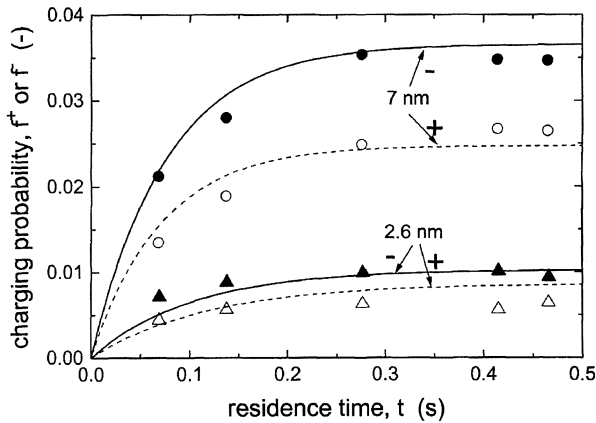
3.4. Charging probability

The charging probability, defined as the fraction of initially neutral particles which acquire a net charge of a given sign upon passing through the charger, has been measured experimentally by a number of authors[28, 30, 32, 35 and 36]. Charging probability increases with time until a steady-state (equilibrium) is reached beyond which the fraction of charged or uncharged particles does not suffer any further modification. Except in our own work[36], charging probabilities have been measured at the steady-state. The experimentally measured probabilities are used in differential mobility analysis to transform the mobility distribution into the required particle size distribution. However, as we have already pointed out before, specially in the case of nanoaerosols one should minimize the extent of particle size modification by diffusion losses and Brownian coagulation, and this implies that we should let the aerosol spend a residence time in the charger as short as is practicable, generally much shorter than the time needed for the particles to attain their steady-state charging condition.

To avoid interference of diffusion losses and coagulation, a careful experimental setup must be devised for the measurement of charging probabilities. In our recent work[36], we used again a series of tube chargers in order to determine the charging probability as a function of time. We did two series of experiments with particles smaller than 10 nm in diameter. In a first series, neutral nanoparticles were charged in the bipolar ion environment of the variable-length charger; in a subsequent set of experiments, we fed bipolarly charged particles to the bipolar charger ("neutralization"). Some typical results of transient probabilities are presented in figures 2 and 3.
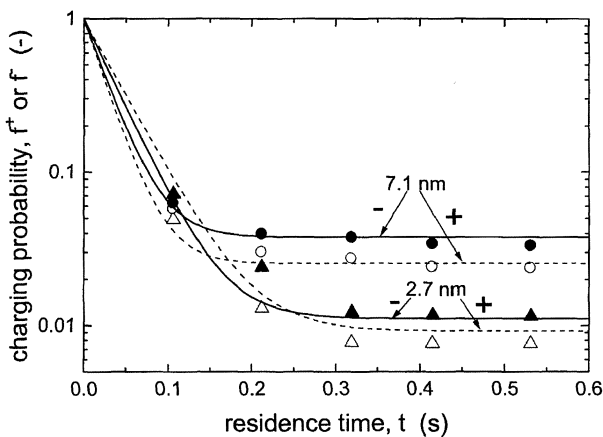
The theoretical curves in figure 2 have been calculated with the analytical solution (14), using Fuchs theory to calculate the ion attachment rate coefficients (equations (24)-(27)). When the aerosol entering the charger is bipolarly charged, an analytical solution similar to (14) can be found using the appropriate initial conditions; such analytical solution is that plotted in figure 3. It is important to note, first, that the time required to attain the steady-state is the same, about 0.3 s, in both processes (charging of neutral particles, and neutralization of charged ones). Also, the steady-state charging probabilities coincide for both cases

Figure 2. Variation of charging probability with residence time in the process of charging of neutral particles. Symbols: experimental data; lines: analytical solution (equation (14)).

Figura 2. Variación de la probabilidad de cargado con el tiempo de residencia en el proceso de cargado de partículas neutras. Símbolos: datos experimentales; curvas: solución analítica (ecuación (14)).

Figure 4. Experimental steady-state charging probabilities for positive particles: □ [28]; ◇ [30]; ▽ [32]; △ [35]; ○ [36]. The curve represents the theoretical charging probability, calculated with equation (19).

Figura 4. Valores experimentales de la probabilidad de cargado en estado estacionario para partículas positivas: □ [28]; ◇ [30]; ▽ [32]; △ [35]; ○ [36]. La curva representa la probabilidad de cargado teórica, calculada con la ecuación (19).
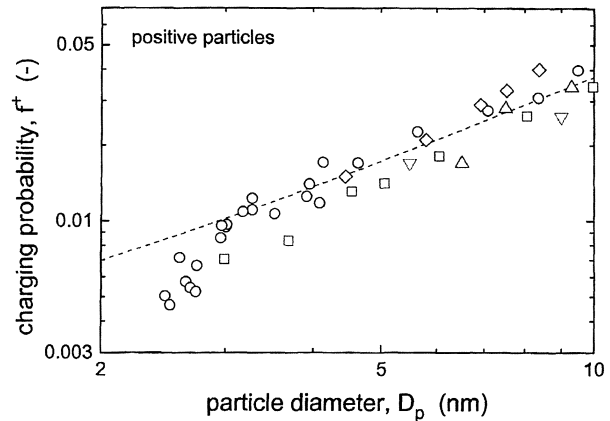

Figure 3. Variation of charging probability with residence time in the process of neutralization of bipolarly charged particles. Symbols: experimental data; lines: analytical solution.

Figura 3. Variación de la probabilidad de cargado con el tiempo de residencia en el proceso de neutralización de partículas cargadas. Símbolos: datos experimentales; curvas: solución analítica.
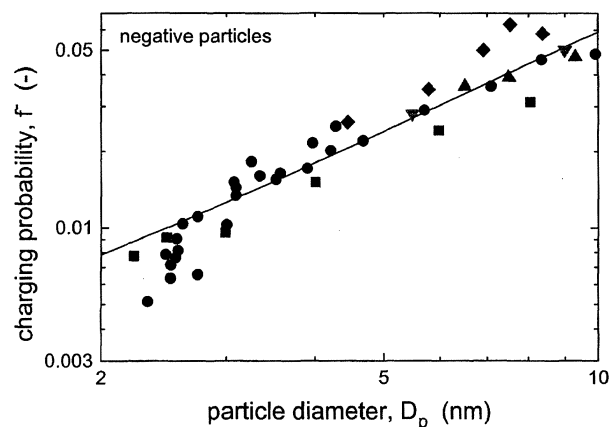

Figure 5. Experimental steady-state charging probabilities for negative particles: □ [28]; ◇ [30]; ▽ [32]; △ [35]; ○ [36]. The curve represents the theoretical charging probability, calculated with equation (19).

Figura 5. Valores experimentales de la probabilidad de cargado en estado estacionario para partículas negativas: □ [28]; ◇ [30]; ▽ [32]; △ [35]; ○ [36]. La curva representa la probabilidad de cargado teórica, calculada con la ecuación (19).

– the whole collection of experimental results can be found in the original paper[36].

The experimentally measured steady-state charging probabilities, obtained by a number of authors, are plotted in figures 4 (positive particles) and 5 (negative particles), along with the theoretically calculated ones using Fuchs theory for the evaluation of the ion attachment rate coefficients. As seen, Fuchs theory gives very good

predictions for particles larger than about 3 nm, as long as the values used for ion mobility and mass (needed to calculate the attachment coefficients) are assumed to be correct. However, somewhat large deviations have been observed for smaller particles, but in the size range below 3 nm, there are very few data – only those of our group[36] – and, therefore, unless more experiments are done

in this extremely small size range, preferably by others, no definitive conclusion should be drawn.

4. CHARGING EFFICIENCY IN AN UNIPOLAR ION ENVIRONMENT

As we have seen, when particle charging is carried out in a bipolar charging environment, such as that existing in a radioactive ionizer, two processes take place simultaneously, namely, charging of neutral particles, and neutralization of those which have become charged. The latter occurs preferentially by attachment of an ion to a particle of opposite polarity, and to a lesser extent through collisions between charged particles of different sign. As a result of the competition between these two processes, charging and neutralization, the fraction of charged particles leaving the ionizer is quite low: the steady-state charged fraction for 10 nm particles is between about 4 % (positive particles) and 6 % (negative particles), and still lower values for smaller particles.

The extremely low nanoparticle charging efficiency of bipolar ionizers can impose practical limitations in experimental works, causing severe measurement errors in the particle sizing and detecting equipments. Therefore, further improvements must obviously be sought through any appropriate modification of the device where particle charging takes place. As commented above, the reason why the charging efficiency of bipolar chargers is so low lies in the fact that recombination (neutralization) of charged particles can not be avoided. The only alternative we are left with is to use unipolar chargers, that is, devices in which aerosol particles collide with ions of only one polarity. The simplest means to achieve an unipolar ion cloud is by DC corona discharge and, in fact, corona ionizers were introduced in differential mobility analysis by Rohmann as far ago as 1923 (cited by Flagan[39]), and later used by a number of researchers (among many others, Langer et al.[40], Liu and Pui[41], and Cheng et al.[42]).
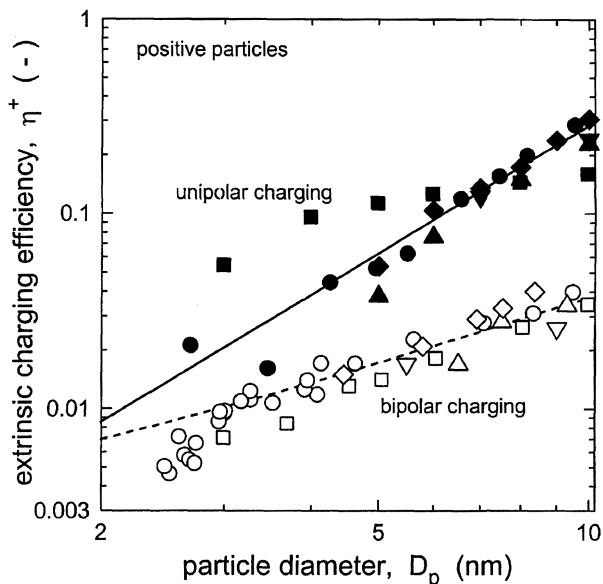
In contrast with the case of bipolar radioactive chargers, it is quite difficult to find in the literature reports concerning the experimental measurement of charging efficiencies for unipolar ionizers. Adachi et al.[43] developed an unipolar radioactive charger in which ions of a given polarity were separated, by means of a relatively weak electric field, from a population of bipolar ions generated by a ^{241}Am source. These authors measured

charging efficiencies for particle diameters above 10 nm. Experimental values of charging efficiency for particles under 10 nm have been reported by Buscher et al.[44] using corona discharge as the ion source, and by Wiedensohler et al.[45], who used a ^{244}Cm to generate bipolar ions in two boxes separated by a charging zone, and an alternating electric field to draw unipolar iones from the boxes into the charging zone. More recently, Chen and Pui[46] have developed a unipolar charger using also radioactive sources and a stream of sheath air surrounding the aerosol in order to reduce particle losses within the charger. These authors, using a sheath-to-aerosol flow rate ratio of 3, obtained extrinsic charging efficiencies (i.e. fraction of neutral particles which carry a net charge after penetrating the charger without having been lost) as high as 65 % for 10 nm particles, measured on a particle number basis. However, in practice one is interested in the number concentration of charged particles at the charger outlet; since in the Chen-Pui charger the aerosol is diluted by a factor of 4, the extrinsic charging efficiencies, on a particle number concentration basis, are actually one fourth of those reported in their article (hence, about 16 % for 10 nm particles). To the best of our knowledge, the latest two developments to date are, first, the unipolar charger of Kruis and Fissan[47], similar to that of Wiedensohler et al.[45] except that the ions in the two generation boxes were produced by corona discharge, instead of by a radioactive source; and a very recent one carried out by our own group[48].

In own experiments[48], we have evaluated the performance of a corona discharge ionizer, consisting basically in a grounded cylindrical tube having a coaxial electrode to which a high dc voltage of either polarity is applied. In this particular case, particle charging takes place by two simultaneous mechanisms, namely, field charging and diffusion charging. For a more detailed description of field charging the reader is referred to the book of Friedlander[49]. On its part, the mechanism of diffusion charging is considerably simpler in this case, because only one ion attachment rate coefficient is involved. Therefore, for nanometer-sized particles, which acquire at most a single charge, the charging rate equation in the presence of unipolar ions of polarity j is simply $df^j / dt = \eta^{j0} f^0 n^j$, from where $f^j = 1-\exp(-\eta^{j0}nt)$. Thus, in theory, all the initially neutral particles become charged at the steady-state. However, this is unattainable in practice, because it would require
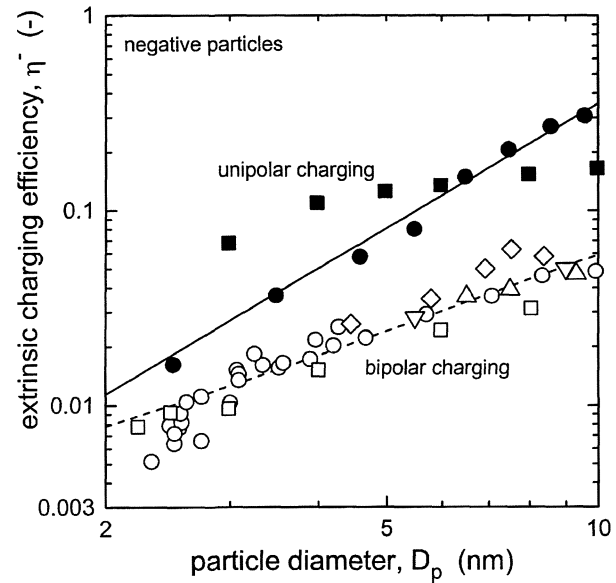
a relatively large aerosol residence time in the charger, during which particles and, specially, ions would be completely lost by diffusion to the walls. That is, the nt product, which controls the charging rate process, is actually decreasing with time and this prevents achievement of too high charging efficiencies.

In the corona type ionizer of our experiments[48], there are also relatively large particle electrostatic losses. It means that not all the particles which acquire a charge can leave the ionizer. This is why, in this particular case, one must consider charging efficiency rather than probability. Different designs result in different efficiencies. Nevertheless, the relative output of charged particles in a corona ionizer is much larger than that attainable in bipolar chargers, as can be seen in figures 6 and 7, where the experimental data of figures 4 and 5 have also been included for comparison. Charging efficiencies in the corona ionizer are much higher, almost an order of magnitude higher for the larger particles tested, than those attainable in bipolar radioactive chargers. For example, for particles about 10 nm in diameter the measured corona charging efficiency was about 0.3 both for positive and negative corona; this should be compared with the

Figure 7. Charging efficiency as a function of particle size for negative particles. Comparison between unipolar charging (■ [46]; ● [48]) and bipolar charging (□ [28]; ◇ [30]; ▽ [32]; △ [35]; ○ [36]).

Figura 7. Eficacia de cargado en función del tamaño de partícula, para partículas negativas. Comparación entre cargado monopolar (■ [46]; ● [48]) y cargado bipolar (□ [28]; ◇ [30]; ▽ [32]; △ [35]; ○ [36]).

corresponding values for the bipolar chargers: 0.04 for positive particles and 0.06 for negative ones. As the particle size decreases, the corona/radioactive charging efficiency ratio decreases but nevertheless is kept well above 2-3 in all the particle size range studied. As already commented, the main reason for this drastic difference lies in the fact that neutralization, i.e. recombination between charged particles of opposite polarity, absent in the case of the unipolar corona ionizer, is the dominant rate process in the radioactive charger – recall that, for a given particle size, the neutralization rate coefficient (ion attachment to a particle of opposite polarity) is between one to two orders of magnitude higher than the charging rate coefficient (ion attachment to a neutral particle).

5. AFTER-CHARGING EFFECTS DOWNSTREAM OF AN AEROSOL NEUTRALIZER

Commercially available bipolar neutralizers are supposed to be designed so as to give a residence time sufficient for the aerosol to attain a steady-state charge distribution. Achievement of a steady-state charge distribution depends essentially on the nt product (ion concentration, residence time in

Figure 6. Charging efficiency as a function of particle size for positive particles. Comparison between unipolar charging (▲ [44]; ▼ [45]; ■ [46]; ◆ [47]; ● [48];) and bipolar charging (□ [28]; ◇ [30]; ▽ [32]; △ [35]; ○ [36]).

Figura 6. Eficacia de cargado en función del tamaño de partícula, para partículas positivas. Comparación entre cargado monopolar (▲ [44]; ▼ [45]; ■ [46]; ◆ [47]; ● [48];) y cargado bipolar □ [28]; ◇ [30]; ▽ [32]; △ [35]; ○ [36];).

51

http://revistademetalurgia.revistas.csic.es

neutralizer). If the concentration of aerosol particles is relatively low in comparison with that of ions, the outlet stream will consist of neutral and charged particles as well as of free ions which have not had the opportunity to come into contact with particles inside the neutralizer, and which can promote further particle charging downstream of the neutralizer. Therefore, not only the aerosol residence time in the neutralizer, but also the aerosol residence time downwind of the neutralizer must be considered. Lack of attainment of steady-state conditions can result in errors when one measures the size distribution of the particles using a differential mobility analyzer (DMA), because transformation of mobility distribution into particle size distribution relies on the assumption that the aerosol has attained a charge equilibrium state.

In principle, the existence of free unattached ions in the exit stream could imply that further charge distribution modification could occur downstream of the ionizer. Whether these *after-charging* effects are present or not was the objective of a recent experimental investigation[50]. The experiments were done with a commercial neutralizer using a ^{85}Kr source, but it is most likely that similar results would be obtained with laboratory-made units or other radioactive sources. (Comparative performance of different neutralizer designs has been reported by Covert *et al.*[51])

From the results of this experimental investigation, the following qualitative conclusions could be drawn. Even when the *nt* product is large enough so that a steady-state charge condition is attained, the equilibrium charged aerosol may still contain free unattached ions, specially when the aerosol concentration is relatively low. In this case, particle charging still continues to take place far beyond the neutralizer outlet but without modification of the aerosol charge distribution, i.e. the rate at which neutral particles become charged after the neutralizer equals that at which charged particles become neutralized. If the equilibrium-charged aerosol containing free ions is mixed with foreign neutral particles, the latter acquire electrical charges while the former keeps its steady-state charge distribution. Obviously, as the *nt* product is reduced, the number concentration of free unattached ions at the neutralizer outlet increases, thus allowing charging of the foreign aerosol to a higher extent.

6. PARTICLE SIZING BY DIFFERENTIAL MOBILITY ANALYSIS

Size-classification of charged aerosol particles by an electric field is of fundamental importance to many fields of aerosol research. On the one hand, it permits the experimental determination of the particle size distribution of aerosols down to the nanometer size range. On the other hand, it enables the separation and continuous extraction of a stream of monodisperse aerosol particles of the desired size from a polydisperse population; the thus generated monodisperse aerosol can then be used to study aerosol processes where particle size plays a key role (e.g., particle size growth by coagulation or condensation, aerosol deposition and filtration, charging, etc.). Indeed, the apparatus with which size-classification is performed, the so-called differential mobility analyzer (DMA), is one of the most practical and useful instruments ever developed in the field of aerosol science.

Several DMA designs have been developed and commercialized. Of these, the most widely used is the concentric cylindrical DMA[41-52]. It consists of two concentric cylindrical electrodes, one of which is grounded (normally the outer electrode), while the other one is connected to a dc power source. It has two flow inlets, one for a stream of filtered dry air (sheath), the other one for the test aerosol stream. Both streams flow laminarly within the annular gap. As soon as the particles enter the DMA near the outer electrode, the charged particles of a given polarity precipitate onto it; the particles of opposite polarity migrate toward the inner electrode while being transported axially by the flowing medium. The migration velocity of the particles depend on their electric mobility and, consequently, on their size, in such a manner that the smallest particles are the first to reach the inner electrode. The inner electrode contains a series of small orifices (*classification port*) near its bottom end, through where particles of a given size (mobility) are withdrawn from the instrument. Particles smaller than those classified precipitate onto the inner electrode upstream of the classification port, while the larger particles leave the DMA without being precipitated or classified (*excess air*). By tuning the strength of the applied electric field one can classify particles of the desired mobility (or size).

The DMA is usually used in combination with (i) a device where aerosol particles are electrically

charged before entering the classification equipment (this has been discussed in depth in the last two sections), and (ii) an instrument to measure the number concentration of the classified particles. The latter can be either an electrometer or, more generally, a condensation nucleus counter[53 and 54].

In the ideal situation in which the particle motion is fully determined by the imposed electric field and the gas flow velocity, the theoretical treatment of the DMA operation is straightforward[41 and 52], and leads to the following equation relating the mean electrical mobility, Z, of the classified particles as a function of the voltage difference V applied between the two concentric electrodes:

$$Z = \frac{q \ln(R_2 / R_1)}{2\pi LV} \qquad (31)$$

In the above expression, q is the flow rate of sheath air, L is the axial distance between the inlet and classification ports, and R_1 and R_2 are the radii of the inner and outer electrodes, respectively. Equation (31) is valid for the usual case in which the DMA is operated in such a manner that the flow rates of inlet and classified aerosol are equal and, hence, the flow rates of sheath and excess air are also equal.

By scanning the applied voltage within a certain range, one can thus obtain the mobility distribution of the charged particles that entered the DMA. From this distribution along with the appropriate theoretical particle charge distribution discussed before, one can then infer the mobility distribution of the original aerosol (i.e. before the ionizer). If wished, one can finally convert the mobility distribution into the particle size distribution by applying the Stokes-Einstein relationship between electrical mobility and particle diameter:

$$D = \frac{kT}{pe} Z = \frac{kTC}{3\pi\mu D_p} \qquad (32),$$

where D is the particle diffusion coefficient, k the Boltzmann's constant, T the absolute temperature, p the number of charges on the particle, e the elementary charge, C the Cunningham slip correction factor, μ the gas viscosity, and D_p the particle diameter. While the above equation is valid for the transition and continuum regimes (particle diameter above about 15 nm), it is not

clear yet whether its applicability can be extended to the free molecular regime[55].

As stated before, equation (31) is valid in the situations where the particle motion is driven by the sheath gas and the external electric field. For particle diameter below about 50 nm, one has to consider also an additional random velocity component arising from the Brownian motion of the particles. The large diffusivity of nanoparticles causes a dramatic deterioration of the DMA performance, a topic that has received much attention during the last 15 years[56-65].

Besides diffusion, another difficulty may appear when attempting to classify too small particles with the DMA. In normal practice, if the aerosol to be measured is highly concentrated it is usual (at least, advisable) to dilute it before size-classification in the DMA. If this is not possible, one has to consider the possibility that the space-charge field developed by the charged particles can be of the same order of magnitude as the applied electric field, in which case the usual electro-hydrodynamic equations describing the DMA operation must be modified in order to infer the actual particle electrical mobility distribution. Space-charge effects in the DMA may arise only in the case of highly-concentrated nanometer-sized particles (it is negligible for large particles – low mobility – because their classification requires large values of the applied electric field). However, the nanometer aerosol particles also undergo a strong Brownian motion superimposed to their deterministic motion as determined by the external force field. Actually, both phenomena, Brownian diffusion and space-charge, must be considered simultaneously. This was done a few years ago by our group[60]; we could solve the relatively complicated resulting equation only after introducing several simplifying assumptions. Later on, we treated the simpler problem in which Brownian diffusion was neglected. In this case, a rigorous solution could be obtained relating the applied electric potential, V′, to the electrical mobility, Z, of the classified particles[66]:

$$V' = V\left(\frac{1}{1+\zeta} + \zeta G\right) \qquad (33)$$

In this expression, V is the required applied voltage in the absence of space-charge effects (equation (31)), G is a function of the flow rates and of some DMA geometric parameters, and:

$$\zeta = \frac{e}{2e_0} NZt \qquad (34),$$

where e is the elementary charge, ε_0 the vacuum permittivity, N the aerosol number concentration, and t the mean aerosol residence time in the DMA. For sufficiently dilute aerosols, $\zeta \to 0$ and, hence, $V' \to V$. From the calculations performed with equation (33) it was concluded that space-charge affects the DMA performance for a value of ζ larger than about 0.02. For instance, for typical values of particle mobility $Z = 0.2$ cm^{2}V^{-1}s^{-1}, and mean residence time $t = 0.25$ s, the above equation predicts that space-charge effects will be noticed for aerosol number concentration above about 5×10^5 cm^{-3}. These predictions were satisfactorily confirmed in a subsequent experimental work[67].

7. NANOMETER AEROSOL REMOVAL BY ELECTRICAL METHODS

Standards of suspended particulate matter emission into the atmosphere are generally expressed on a mass basis. Given that particle mass increases with the third power of particle size, the presence of nanometer particles in industrial gas exhausts is often neglected because their contribution to the total emitted mass is rather insignificant. However, a negligible mass of nanometer particles can amount for quite a large number of particles, which should not be overlooked for the reasons explained in the Introduction.

Therefore, one should not be satisfied stating that a given particle filtration equipment has a mass collection efficiency of, say, more than 95 %. To be more precise, consider a typical electrostatic precipitator, one of the most widely used particle collection devices. In this equipment, particle collection relies on the capability of the particles to become electrically charged by the ions generated in the corona discharge. As we have seen, particle charging efficiency (i.e. the number fraction of originally neutral particles which acquire one or more electrical charges in the corona field) increases with particle size in such a manner that one can safely assume that, provided the design and the operating conditions of the corona discharge are appropriate, practically all the particles larger than about 50 nm become charged and can thus be deposited on the collecting electrode. However, as particle size decreases electrical charging becomes more and more difficult, so that most of the particles below about

10 nm remain uncharged and thus penetrate the electrostatic precipitator without being collected. Some recent experimental works on electrostatic precipitators have shown indeed a sharp decrease in the collection efficiency for particles smaller than 50 nm[68-71].

The strong Brownian motion of the smallest particles makes them depart erratically from the gas streamlines and, as a consequence, these particles can be easily intercepted by any obstacle present in the flow system (a fiber, for instance). The collection efficiency by the mechanism of Brownian diffusion increases as the particle size decreases[72-74]; actually, Brownian diffusion is the only mechanism by which particles of a few nanometers in size can be efficiently captured. Therefore, a particle collection equipment in which the two mechanisms, diffusional and electrostatic deposition, act simultaneously, can be an attractive means to capture efficiently the suspended particles regardless of their size. There exists a number of commercial filters based on these principles and employing various geometries and types of mechanical filtering media, but experimental data about their performance often consists of global mass efficiencies, in many cases without consideration of the dependency of the filtration efficiency on particle size. Therefore, the actual nanoparticle collection efficiency of these types of combined filters is yet unknown.

Recently, we have developed a laboratory-scale prototype of such an equipment, and carried out a preliminary experimental evaluation of its performance[75]. Our diffusion-electrostatic precipitator consists of a cylinder containing a set of wire screens at its rear end, and three coaxial electrodes. Upon corona discharge, most of the larger particles acquire a charge and are electrostatically deposited onto the grounded screens; on its part, most of the smallest particles remain neutral (hence, they do not undergo electrostatic precipitation) but can be intercepted by the wires of the screens. The combination of both mechanisms, electrostatic and diffusion, has proved to be an efficient means to collect particles with diameters down to 3 nm (see Fig. 8).

Obviously, this device would present the problem of screen clogging, which would make this filter impractical to use for a long period or for too concentrated aerosols; the diffusion-electrostatic precipitator should, in that case, be considered as an after-filter to collect the smallest particles
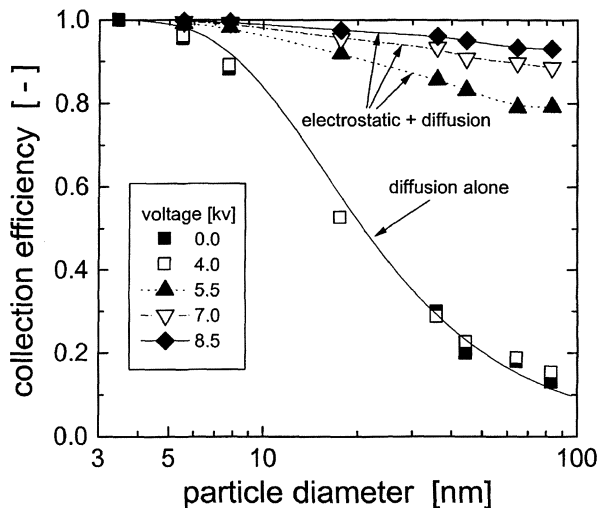
Figure 8. Collection efficiency as a function of particle size and voltage difference between electrodes and screens, in an electrostatic-diffusion precipitator. Aerosol face velocity: 0.2 ms^{-1}.

Figura 8. Eficacia de captura en función del tamaño de partícula y de la diferencia de potencial entre los electrodos y las mallas, en un precipitador electrostático-difusivo. Velocidad del aerosol: 0,2 ms⁻¹.

which can not be captured by conventional equipments.

Aerosol filtration efficiency can also be greatly enhanced by the presence of electric charges on the filtering medium, regardless the charging state of the particles. Electrect filters, i.e. filters having a permanent electric charge[76], are widely used in air cleaning applications requiring high filtration efficiency. In these filters, both charged and neutral particles are captured by electrical forces in addition to other conventional mechanisms such as interception, inertial impaction and diffusion. In some instances, filtration efficiency may deteriorate with time as the filter is loaded with particles[77]. We developed a somewhat similar filtration device for the collection of nanometer-sized particles. The device consists basically in a grounded metal cylinder with a dielectric screen, which is initially discharged. Experiments were carried out with two types of monodisperse unipolarly charged particles having different dielectric constants (Ag and NaCl) and mobility-equivalent particle diameters between 2 and 10 nm (Peclet number between 4 and 80). At the very beginning of the process, the screen is uncharged and filtration is controlled by particle diffusion. As the number of charges on the screen increases due to the diffusional deposition of charged particles, an electric field of increasing strength is developed

between the dielectric screen and the conductive metallic walls of the cylinder where the screen is placed. As a result, particles are also driven and lost to the walls and collection efficiency increases. This transient process can be well described by two dimensionless parameters, namely the Peclet number Pe, and a non-dimensional number N_C expressing the ratio of the particle drift velocity due to the field to the particle convective velocity due to the flowing medium (air). From the experimental data, the following correlation for the collection efficiency E could be obtained[78]:

$$E = 1 - \exp\left[-S(2.7\text{Pe}^{-2/3} + 3.73\text{Pe}^{-1/2}N_C^{2/3})\right] \quad (35),$$

where S is the so-called screen parameter, which includes all the relevant geometry of the screen.

8. CONCLUDING REMARKS

The present review has been devoted to recent fundamental research concerning the electrical charging of nanometer-sized aerosol particles, with special emphasis on the work performed by the authors and their former colleagues. The topics treated are, in general, quite relevant to aerosol processing and measurement. In contrast with aerosols of relatively large particle size, the electrical behavior of nanometer aerosols has not received much attention in the past, mainly because no adequate instrumentation was yet available, and it is only very recently that such an study has been initiated. Clearly, much more research efforts are required in order to understand in more depth the fundamental physical behavior of such extremely small particles, specially nowadays that an increasing interest is being placed on the applications of nanoparticles in diverse fields of science and technology.

Acknowledgments

REFERENCES

[1] D.Y.H. PUI and D.R. CHEN, *J. Aerosol Sci.* 28 (1997) 539-544.

[2] A. GURAV, T. KODAS, T. PLUYM and Y. XIONG, *Aerosol Sci. Technol.* 19 (1993) 411-452.

[3] K.A. KUSTERS and S.E. PRATSINIS, *Powder Technol.* 82 (1995) 79-91.

[4] M. ALONSO and F.J. ALGUACIL, *Rev. Metal. Madrid* 37 (2001) 693-712.

[5] R.L. DAVISON, D.F.S. NATUSCH, J.R. WALLACE and D.C. EVANS, *Environ. Sci. Technol.* 8 (1974) 1107-1113.

[6] W.P. LINAK and T.W. PETERSON, *Symp. (Int.) Combust.* 21 (1986) 399-410.

[7] R.C. FLAGAN and J.H. SEINFELD, *Fundamentals of Air Pollution Engineering*, Prentice Hall, Englewood Cliffs, 1988, p. 359.

[8] E.I. KAUPPINEN and T.A. PAKKANEN, *Environ. Sci. Technol.* 24 (1990) 1811-1818.

[9] E. CEREDA, G.M. BRAGA, M. PEDRETTI, G.W. GRIME and A. BALDACCI, *J. Aerosol Sci.* 27 (1996) 607-619.

[10] J. ONDOV and A. WEXLER, *Environ. Sci. Technol.* 32 (1998) 2547-2555.

[11] P. BISWAS and C.Y. WU, *J. Air Waste Manag. Assoc.* 48 (1998) 113-127.

[12] G.M. HIDY, *Aerosols: an Industrial and Environmental Science*, Academic Press, Orlando, 1984, pp. 601-624.

[13] G. OBERDORSTER, J. FERIN, G. FINKELSTEIN, P. WADE and N. CORSON, *J. Aerosol Sci.* 21 (1990) 384-387.

[14] C.R. MILLER, P. BISWAS and G.D. LEIKAUF, *Aerosol Sci. Technol.* 35 (2001) 829-839.

[15] D.R. CHEN, D.Y.H. PUI, D. HUMMES, H. FISSAN, F.R. QUANT and G.J. SEM, *J. Aerosol Sci.* 29 (1998) 497-509.

[16] P. KULKARNI, N. NAMIKI, Y. OTANI and P. BISWAS, *J. Aerosol Sci.* 33 (2002) 1279-1296.

[17] Y. ENDO, M. ALONSO, H. ICHITSUBO, T. HASHIMOTO and Y. KOUSAKA, *J. Aerosol Sci.* 27 (1996) 511-518.

[18] W.A. HOPPEL and G.M. FRICK, *Aerosol Sci. Technol.* 5 (1986) 1-21.

[19] W.H. MARLOW and J.R. BROCK, *J. Colloid Interface Sci.* 50 (1975) 32-38.

[20] R. GUNN, *J. Meteorology* 11 (1954) 329-347.

[21] H.R. PRUPPACHER and J.D. KLETT, *Microphysics of Clouds and Precipitation*, Kluver, Dordrecht, 1997, p. 800.

[22] C.F. CLEMENT, *Physical and Chemical Properties of Aerosols*, ed. I.Colbeck, Blackie, London, 1998, pp. 205-218.

[23] M. ALONSO, A. HERNÁNDEZ-SIERRA and F.J. ALGUACIL, *J. Phys. A: Math. Gen.* 35 (2002) 6271-6280.

[24] Y.S. MAYYA and B.K. SAPRA, *J. Aerosol Sci.* 27 (1996) 1169-1178.

[25] N.A. FUCHS, *Z. Phys.* 89 (1934) 736-744.

[26] J. BRICARD, *J. Geophys. Res.* 54 (1949) 39-46.

[27] N.A. FUCHS, *Geofis. Pura Appl.* 56 (1963) 185-193.

[28] G.P. REISCHL, J.M. MAKELA, R. KARCH and J. NEcid, *J. Aerosol Sci.* 27 (1996) 931-949.

[29] V.A. MOHNEN, *Electrical Processes in Atmospheres*, ed. H.Dolezaleck and R. Reiter, D Steinkopff, Darmstadt, 1977, pp. 1-17.

[30] A. HUSSIN, H.G. SCHEIBEL, K.H. BECKER, and J. PORSTENDORFER, *J. Aerosol Sci.* 14 (1983) 671-677.

[31] H.Y. WEN, G.P. REISCHL and G. KASPER, *J. Aerosol Sci.* 15 (1984) 89-102.

[32] M. ADACHI, Y. KOUSAKA and K. OKUYAMA, *J. Aerosol Sci.* 16 (1985) 109-123.

[33] A. WIEDENSOHLER, E. LUTKENMEIER, M. FELDPAUSCH and C. HELSPER, *J. Aerosol Sci.* 17 (1986) 413-421.

[34] W.A. HOPPEL and G.M. FRICK, *Aerosol Sci. Technol.* 12 (1990) 471-496.

[35] A. WIEDENSOHLER and H. FISSAN, *Aerosol Sci. Technol.* 14 (1991) 358-364.

[36] M. ALONSO, Y. KOUSAKA, T. NOMURA, N. HASHIMOTO and T. HASHIMOTO, *J. Aerosol Sci.* 28 (1997) 1479-1490.

[37] A.V. FILIPPOV, *J. Aerosol Sci.* 24 (1993) 423-436.

[38] M. ALONSO, T. HASHIMOTO, Y. KOUSAKA, M. HIGUCHI and T. NOMURA, *J. Aerosol Sci.* 29 (1998) 263-270.

[39] R.C. FLAGAN, *Aerosol Sci. Technol.* 28 (1998) 301-380.

[40] G. LANGER, J. PIERRARD and G. YAMATE, *Int. Journal Air Water Poll.* 8 (1964) 167-176.

[41] B.Y.H. LIU and D.Y.H. PUI, *J. Aerosol Sci.* 6 (1975) 249-264.

[42] S.H. CHENG, M.B. RANADE and J.W. GENTRY, *Aerosol Sci. Technol.* 26 (1997) 433-446.

[43] M. ADACHI, Y. KOUSAKA and K. OKUYAMA, *J. Aerosol Sci.* 16 (1985) 109-123.

[44] P. BUSCHER, A. SCHMIDT-OTT and A. WIEDENSOHLER, *J. Aerosol Sci.* 25 81994) 651-663.

[45] A. WIEDENSOHLER, P. BUSCHER, H.C. HANSSON, B.G. MARTINSSON, F. STRATMANN, G. FERRON and B. BUSCH, *J. Aerosol Sci.* 25 (1994) 639-649.

[46] D. R. CHEN and D.Y.H. PUI, *J. Nanopoarticle Res.* 1 (1999) 115-126.

[47] F.E. KRUIS and H. FISSAN, *J. Nanoparticle Res.* 3 (2001) 39-50.

[48] A. HERNÁNDEZ-SIERRA, F.J. ALGUACIL and M. ALONSO, *J. Aerosol Sci.* submitted.

[49] S.K. FRIEDLANDER, *Smoke, Dust and Haze*, Oxford University Press, New York, 2000, pp. 40-50.

[50] M. ALONSO, F.J. ALGUACIL, T. NOMURA and Y. KOUSAKA, *J. Aerosol Sci.* 32 (2001) 287-294.

[51] D. COVERT, A. WIEDENSOHLER and L. RUSSELL, *Aerosol Sci. Technol.* 27 (1997) 206-214.

[52] E.O. KNUTSON and K.T. WHITBY, *J. Aerosol Sci.* 6 (1975) 443-460.

[53] J.K. ARGAWAL and G.J. SEM, *J. Aerosol Sci.* 11 (1980) 343-357.

[54] Y. KOUSAKA, T. NIIDA, K. OKUYAMA and H. TANAKA, *J. Aerosol Sci.* 13 (1982) 231-240.

[55] H. TAMMET, *J. Aerosol Sci.* 26 (1995) 459-475.

[56] Y. KOUSAKA, K. OKUYAMA, M. ADACHI and T. MIMURA, *J. Chem. Eng. Jpn.* 19 (1986) 401-407.

[57] M.R. STOLZENBURG, Ph.D. Thesis, University of Minnesota, 1988.

[58] J. ROSELL-LLOMPART, I.G. LOSCERTALES, D. BINGHAM and J. FERNÁNDEZ DE LA MORA, *J. Aerosol Sci.* 27 (1996) 695-719.

[59] S.H. ZHANG and R.C. FLAGAN, *J. Aerosol Sci.* 27 (1996) 1179-1200.

[60] M. ALONSO and Y. KOUSAKA, *J. Aerosol Sci.* 27 (1996) 1201-1225.

[61] M. ALONSO, Y. KOUSAKA, T. HASHIMOTO and N. HASHIMOTO, *J. Aerosol Sci.* 29 (1998) 985-994.

56

[62] I.G. LOSCERTALES, *J. Aerosol Sci.* 29 (1998) 1117-1139.

[63] HAGWOOD, Y. SIVATHANU and G. MULHOLLAND, *Aerosol Sci. Technol.* 30 (1999) 40-61.

[64] R.C. FLAGAN, *Aerosol Sci. Technol.* 30 (1999) 556-570.

[65] J. SALM, *Aerosol Sci. Technol.* 32 (2000) 602-612.

[66] M. ALONSO, F.J. ALGUACIL and Y. KOUSAKA, *J. Aerosol Sci.* 31 (2000) 233-247.

[67] M. ALONSO, F.J. ALGUACIL, Y. WATANABE, T. NOMURA and Y. KOUSAKA, *Aerosol Sci. Technol.* 35 (2001) 921-923.

[68] T. WATANABE, F. TOCHIKOBU, Y. KOIZUMI, T. TSUCHIDA, J. HAUTANEN and I.E. KAUPPINEN, *J. Electrost.* 34 (1995) 367-383.

[69] K.H. YOO, J.S. LEE and M.D. OH, *Aerosol Sci. Technol.* 27 (1997) 308-323.

[70] K.J. BOELTER and J.H. DAVIDSON, *Aerosol Sci. Technol.* 27 (1997) 689-708.

[71] Y. ZHUANG, Y.J. KIM, T.G. LEE and P. BISWAS, *J. Electrost.* 48 (2000) 245-260.

[72] Y.S. CHENG and H.C. YEH, *J. Aerosol Sci.* 11 (1980) 313-320.

[73] M. ALONSO, Y. KOUSAKA, T. HASHIMOTO and N. HASHIMOTO, *Aerosol Sci. Technol.* 27 (1997) 471-480.

[74] M. ALONSO, F.J. ALGUACIL and T. NOMURA, *J. Aerosol Sci.* 32 (2001) 1359-1367.

[75] M. ALONSO and F.J. ALGUACIL, *J. Air Waste Manag. Assoc.* 52 (2002) 1342-1347.

[76] F.J. ROMAY, B.Y.H. LIU and S.J. CHAE, *Aerosol Sci. Technol.* 28 (1998) 224-234.

[77] D.C. WALsh and J.I.T. STENHOUSE, *J. Aerosol Sci.* 28 (1997) 307-321.

[78] M. ALONSO and F.J. ALGUACIL, *J. Colloid Interface Sci.* 216 (1999) 71-76.